



HAL
open science

A combinatorial optimisation approach to energy management strategy for a hybrid fuel cell vehicle

Stéphane Caux, Yacine Gaoua, Pierre Lopez

► To cite this version:

Stéphane Caux, Yacine Gaoua, Pierre Lopez. A combinatorial optimisation approach to energy management strategy for a hybrid fuel cell vehicle. *Energy*, 2017, 133, pp.219-230. 10.1016/j.energy.2017.05.109 . hal-01531987

HAL Id: hal-01531987

<https://hal.science/hal-01531987>

Submitted on 2 Jun 2017

HAL is a multi-disciplinary open access archive for the deposit and dissemination of scientific research documents, whether they are published or not. The documents may come from teaching and research institutions in France or abroad, or from public or private research centers.

L'archive ouverte pluridisciplinaire **HAL**, est destinée au dépôt et à la diffusion de documents scientifiques de niveau recherche, publiés ou non, émanant des établissements d'enseignement et de recherche français ou étrangers, des laboratoires publics ou privés.

A Combinatorial Optimisation Approach to Energy Management Strategy for a Hybrid Fuel Cell Vehicle

Stéphane Caux

LAPLACE, Université de Toulouse, CNRS, INPT, UPS, Toulouse, France

Yacine Gaoua

LAAS-CNRS, Université de Toulouse, CNRS, Toulouse, France

LAPLACE, Université de Toulouse, CNRS, INPT, UPS, Toulouse, France

Pierre Lopez

LAAS-CNRS, Université de Toulouse, CNRS, Toulouse, France

Abstract

Hybrid Electric Vehicles are becoming more and more prevalent for economic and environmental reasons. Many studies have been conducted in order to improve Hybrid Electric Vehicle performance by increasing their autonomy while respecting the power demand of the electric motor and various constraints. Focusing on the Hybrid Electric Vehicle energy management problem, different approaches and strategies already exist based on non-linear modelling, selection of adequate architecture and source design or the expertise of the manufacturer in the domain. In this paper, a new combinatorial approach is presented to optimally manage offline Hybrid Electric Vehicle energy distribution, composed of two energy sources: a fuel cell as a main source and a super-capacitor for energy storage. New mathematical mod-

Email addresses: caux@laplace.univ-tlse.fr (Stéphane Caux),
y.gaoua@yahoo.com (Yacine Gaoua), pierre.lopez@laas.fr (Pierre Lopez)

elling has been developed that reflects the functioning of the Hybrid Electric Vehicle energy chain, using an exact method to provide an optimal solution that corresponds to hydrogen consumption. Simulations were performed on different realistic mission profiles that showed a significant gain in solution quality and computation time compared with other approaches presented in the literature. Since the quality of solutions depends on the reliability of input data, including disruptions, a robustness study also is carried out.

Keywords: Fuel Cell Vehicle, Energy Management, Global Optimisation, Combinatorial Approach, Integer Linear Programming, Robustness.

1. Introduction

On Earth, more than one billion cars circulate today, and manufacturers produce more than 80 million new vehicles every year [1], in addition to other means of transport, nearly all propelled by an Internal Combustion Engine (ICE) with conventional energy (gas and oil). A huge amount of carbon dioxide particles is released daily in the atmosphere, that is harmful to human health and to the environment. The public, better informed of climate change risks by extensive literature, and the scientific community now are organised to put pressure on political and economic decision-makers to take appropriate measures to counteract this threat and promote energy transition. Car manufacturers contributing to this policy, as well, invest in research and development of new vehicle prototypes with hybrid or full electrical energy traction [2].

Even though the first Hybrid Electric Vehicle (HEV) was conceived at the end of 19th century, the low autonomy and the important mass of elec-

tric vehicles encouraged the industry to develop and use ICE, since oil was available, affordable and the number of vehicles was low. Over time and because of rising oil prices and abnormal rate of CO_2 emissions in the air, car manufacturers and researchers conducted a lot of research in order to commercialise a new generation of HEVs equipped with renewable energy sources with a better performance.

The energy management field is very large, also in transportation applications. Actually, many research works deal with solving to optimality energy and power delivered by several decentralised sources, most of them using renewable energy sources. Hydrogen and Fuel Cell are promising in such mobile systems. The optimal problem is more complex when the design-case and the use-case are mixed.

In [3], it can be noticed it is more convenient to separate two problems depending on the time horizon. For a long term, energy management can be driven with criteria depending on prediction, cost of investment and infrastructure and sizing optimization steps. A real-time energy management is requested for an optimal power split on-board subject to power and energy constraints using given sizing elements and power train architecture; all studies for plug-in HEV or linking HEV to the grid are specific too.

In [4], it can be seen the strategy will be different and also the optimisation criterion can be different. In HEV traction case, the power demand has to be delivered (no scheduling and no peaks cancelling policy are possible). A global optimisation is thus possible knowing the power flow characteristics and the entire mission profile. A global optimum is reached subject to energy minimization all over the known trip.

In this paper, a particular hybrid structure of an electric vehicle with two sources is considered: Fuel Cell (FC) as a main source of electrical energy used for the propulsion of the vehicle (called a powertrain or traction chain), and a pack of super-capacitors for energy storage used to support the FC during traction phases. The goal is to improve vehicle autonomy with the knowledge of the mission profile to achieve. Nevertheless, offline smart energy management is crucial if the demands of the electrical engine are to be met while respecting different HEV constraints related to system function, safety conditions, and sources design.

Different approaches were studied in previous works, in order to manage energy distribution for the same type of traction chain and increase its autonomy by minimising fuel consumption by the main source. Among these approaches, the most cited in the literature is undoubtedly Dynamic Programming, used offline when the mission profile is known [5]. This method, based on Bellman's principle after the discretisation of the energy space of the storage system [6], reveals some weaknesses related to the choice of the discretisation step-size that significantly affects computation time and decision quality. Another method frequently cited in this problematic is an Optimal Control approach [7] based on Pontryagin's minimum principle and the calculation of derivatives of the Hamiltonian function [8] or the reporting of all source consumptions in an equivalent space where optimal control is conducted (equivalent consumption management strategy [9]). This method induces polynomial approximation, which generates some errors and does not take into account some saturation constraints due to the limitation in sources design. Moreover, parameter setting to satisfy the state of energy

constraints is somehow tricky.

Recently, much work has been carried out, mainly to accurately solve the global optimisation problem offline when the mission is known (based on multi-level [3], simulated annealing [4], quasi-Newton method [6]) or by using artificial intelligence approaches (*e.g.*, Particle Swarm Optimisation [10]). Other methods are preferred in the literature with real-time on-line implementation objectives: an on-line optimal control approach [11] with an adaptive principle (equivalent consumption minimisation strategy – ECMS [12]) or heuristics and rule-based approaches (Fuzzy Logic [13] and type-II optimized Fuzzy Logic [14] possibly in combination with a genetic algorithm [15] or adding an adaptive mechanism [16]), in order to minimise hydrogen consumption by the fuel cell system. Control strategies based on load following also have been experimented in [17]. The solutions obtained by these approaches are suboptimal due to their non-linear formulation of the problem or the setting of some parameters generally involving important computation times.

In the work presented in this paper, the above state-of-the-art approaches are exploited with the objective of comparing them with the new propositions. Therefore, a new approach is proposed to address the best power set points for the HEV system in order to manage energy distribution and minimise hydrogen consumption with a reduced computation time. It consists of proposing a new linear modelling, which is then solved to optimality by using Integer Linear Programming. To speed up the optimisation process, cutting planes are added to the original formulation to reduce the search space. The problem is formulated in this paper as a combinatorial problem using set

points corresponding to data representing the source behaviours subject to constraints of power and energy limits and consumption minimisation. This approach is new and very different from classical studies because there is no need of derivative functions nor polynomial approximations. (Mixed-)Integer
95 Linear Programming can be used to solve approximate linearized problem, however the proposed formulation overcomes some drawbacks, provides the optimum and is less time consuming to be implemented in real time on-board. The optimal solution is the series of optimal set points to follow the mission with the minimum consumption cost defined. To measure the sensitivity of
100 the problem against input data disruptions, a robustness study is performed to achieve a worst-case solution to be valid regardless of the scenario. Simulations based on several realistic mission profiles illustrate the improvement using the novel modelling.

The paper is organised as follows: First, Section 2 presents the different
105 sources and components that constitute the HEV energy chain. Then Section 3 provides a survey of the most used approaches in the literature that address this problem. This section provides basis results from which it will be possible to draw comparisons with the new proposed approach. Section 4 is devoted to the proposed contribution using new mathematical modelling and approaches
110 in order to reach better power references to optimally manage HEV energy distribution. Results of simulations on realistic mission profiles to illustrate the performance are presented in Section 5, followed by a robustness study in Section 6.

2. Hybrid vehicle structure

115 The HEV energy chain under study consists of two energy sources with a series hybrid configuration, which means that two contributions are added onto an electrical node before feeding the electrical moto-propulsion group, as shown in Figure 1.

INSERT FIGURE 1 ABOUT HERE

120 A Fuel Cell Stack (FCS) represents the main source producing energy via the chemical reaction of hydrogen and oxygen. It is characterised by its high efficiency, which exceeds 40% (mainly limited to compressor and ancillary losses) [18], generating electrical energy with little fuel, unlike the performance of ICE, which varies between 25% and 30% [19]. It should be
125 noted that the energy converted by FCS also emits water steam and heat, which can be used as a secondary need. This aspect of cogeneration potential is not treated in this paper.

The FCS efficiency curve shown in Figure 2 is based on experimental measurements. It is expressed under a fixed cathodic pressure and a fixed temperature and measurements establishing a unique polarisation curve. This
130 quantity, denoted by η_{fcs} , corresponds to the entire stack, thus is computed using the static fuel cell core efficiency η_{fc} , which can be given by the manufacturer or by measurements [15], the efficiency of their ancillaries such as an air compressor¹ $\eta_{compressor}$, and the efficiency of the embedded in the

¹Air compressor represents 80% of the energy consumed by all the FCS ancillaries (air compressor, temperature and humidification regulating pumps, converter, etc.).

135 stack buck-boost converter² η_{cvs} , which connects it to the distribution bus.
 It yields:

$$\eta_{fcs} = \eta_{fc} \cdot \eta_{compressor} \cdot \eta_{cvs} \quad (1)$$

INSERT FIGURE 2 ABOUT HERE

In this paper, the efficiency curve used shows that maximum FCS efficiency can reach 46% when the FCS provides around 24 kW [10].

140 The energy chain also includes a Storage Element (SE) composed of a pack of super-capacitors, which can support the FCS in the acceleration phases to obtain a better performance of the overall traction chain and can be recharged during vehicle braking phases (reversible element). The SE is characterised by its storage capacity E_{nom} and its power losses shown in Figure 2b, denoted by $Loss_{se}$. SE power losses are computed using buck-boost converter losses $Loss_{cvs}$ and power lost by the super-capacitors pack $R_{sc}I_{sc}^2$, where I_{sc} corresponds to the current flowing through the super-capacitors pack, and R_{sc} its equivalent resistor, which has a non-linear form (not the same in charge and discharge mode).

$$Loss_{se} = Loss_{cvs} + R_{sc}I_{sc}^2 \quad (2)$$

150 3. Mathematical modelling

The objective is to minimise hydrogen consumption used by the FCS throughout the mission, while satisfying system constraints. Many studies have been

²The converter is an electronic module delivering a current to maintain with intern control loops the bus voltage to its reference despite voltage variations of the FCS and the storage system. It is characterised by its high efficiency, ranging from 93% to 97%.

realised on non-linear modelling due to source characteristics (FCS efficiency and SE power losses), using the following modelling:

$$\min \sum_{t=1}^T P_h(t) \Delta t \equiv \min \sum_{t=1}^T \frac{P_{fcs}(t)}{\eta_{fcs}(P_{fcs}(t))} \Delta t \quad (3)$$

$$P_{fcs}(t) + P_{se}(t) \geq P_{req}(t) \quad \forall t \in T \quad (4)$$

$$0 \leq P_{fcs}(t) \leq P_{fcs}^{max} \quad \forall t \in T \quad (5)$$

$$P_{se}^{min} \leq P_{se}(t) \leq P_{se}^{max} \quad \forall t \in T \quad (6)$$

$$SoE^{min} \leq SoE(t) \leq SoE^{max} \quad \forall t \in T \quad (7)$$

$$SoE(t) = SoE(t-1) - P_s(t) \Delta t \quad \forall t \in T \quad (8)$$

$$P_s(t) = P_{se}(t) + Loss_{se}(P_{se}(t)) \quad \forall t \in T \quad (9)$$

$$SoE(T) = SoE(0) \quad (10)$$

155 T is the time horizon (mission duration). The decision variables of the problem are: $P_{fcs}(t)$ the power provided by the FCS at time t , $P_{se}(t)$ the power provided/recovered (positive/negative) by the SE at time t , and $SoE(t)$ the state of energy of the SE at time t . Input data of the problem are defined in Table 1. Consequently, the meaning of the mathematical model is
160 as follows:

- (3): The objective function is to minimise the hydrogen consumption used by the FCS; it also can be written using the FCS efficiency and the power it provides. Hydrogen quantities P_h are calculated using the operating points of the fuel cell efficiency (experimental data sheet),
165 $P_h = P_{fcs}/\eta_{fcs}$. Then, the numerical equation of the objective function is achieved using a 15-degree polynomial taking into account the

minimisation of the approximation errors.

- (4): Demand satisfaction of the powertrain when the vehicle is accelerating. The vehicle also recovers energy during braking phases via the transformation of the kinetic energy into electrical energy. However, recovering all braking energy can force the FCS to operate at poor efficiency: for example, when the mission profile begins with a descent and the driver brakes, this leads to the recovery of braking energy, or the saturation of the storage element, hence the importance of relaxation of $P_{fcs}(t) + P_{se}(t) = P_{req}(t)$ using inequalities (4).
- (5) and (6): Power limits related to the design of the energy sources.
- (7): Storage capacity of the storage element. Generally, SE only can be used between 25% and 100% of its energy capacity.
- (8): State of energy computation using previous state of energy and recovered energy.
- (9): Energy losses of the storage element used to identify the real power $P_s(t)$ supplied/recovered by the storage element.
- (10): This constraint can be optionally added, meaning that the final state of energy of the storage system should be reloaded to its original level at the end of the mission. This constraint makes it possible to go from mission to mission without charging the storage system.

INSERT TABLE 1 ABOUT HERE

To find the solution of the present problem, which corresponds to the consumption of hydrogen minimisation, mission profiles are proposed by the French Institute of Science and Technology for Transport, Development and Networks (<http://www.ifsttar.fr/en/welcome/>). The INRETS mission profile corresponds to the instantaneous HEV power demand in urban areas shown in Figure 3a, the ESKISEHIR mission profile associated with a tramway power demand in Turkey (Figure 3b), and three other mission profiles, Figures 3c, 3d, 3e, that correspond to urban, road and highway power measurements. Each mission is characterised by its duration T , its sampling step Δt and the different operation modes such as traction (resp. braking or stop mode) when the demand is positive (resp. negative or zero).

INSERT FIGURE 3 ABOUT HERE

All figures describe different missions followed by a HEV. These data are not only used to feed the study with actual trips but also highlight various types of requests. Thus, figures show missions with partial part repetition, the presence or absence of stop phases, high dynamics (power variation / time) or low/high positive and/or negative magnitude.

To solve the non-linear programming problem, many approaches and methods have been implemented for purposes of comparison: dynamic programming (DP), quasi-Newton method (QN), fuzzy logic (FL), etc., which make it possible to find a suboptimal solution as shown in Table 2 due to the polynomial approximation used in a QN approach or by the setting of parameters for a DP and FL approach (FL membership functions are optimally placed by offline supervision using genetic algorithms, while the form

and number of chosen membership functions allow the problem to be defined accurately) [14].

INSERT TABLE 2 ABOUT HERE

215 The solution provided by a QN method is better in terms of solution quality and computation time, while respecting the constraint of the final state of energy. The DP approach is an exact method, but it depends on the choice of the step discretisation, which significantly impacts solution performance and computation time. It also should be noted that while the solution provided by an FL approach is good, the solution is calculated without taking
220 into account the final state of energy constraint. This approach is efficient in a real-time strategy, but the setting of the fuzzy parameters in order to obtain a good solution requires offline optimisation, which itself requires long computation times.

225 The new combinatorial model will overcome these drawbacks because the combinatorial optimisation only selects one point among a set of points and returns the best sequence of points to follow to reach the minimum consumption.

Table 2 compares optimal consumptions obtained with the three “classical” methods on five mission profiles we compare here after to the new results
230 obtained on the same missions.

In order to compare the performance of the solutions obtained with the new approach developed (see Section 5), the best solution provided by the QN method is used when the constraint of the final state of energy is taken
235 into account, and FL is used for real-time computation when this constraint

is deactivated. CPU times indicated depend on the processor, memory and programming environment used, but is interesting for relative comparison to discriminate among the different methods.

FL is a real-time optimisation approach (instantaneous optimisation, each
240 time step) while the QN method is a global optimisation approach, which explains the consumption gap and the advantage of the QN method. To improve FL modelling, different fuzzy membership functions (more non-linear) can be used thereby increasing the time-setting procedure and badly impacting on-line implementation. Now that the results and drawbacks of such
245 previous models and methods have been highlighted, the new combinatorial approach can be proposed. All derivative, approximation and sampling drawbacks are cancelled in this new combinatorial modelling driven by experimental data set-points to be optimally chosen.

4. New combinatorial approach

250 In this section, an original model for a HEV energy management is proposed. Modelling the problem as a linear program enables us to obtain an optimal solution using exact methods of operations research such as Branch-and-Bound or Branch-and-Cut procedures [20].

The principle of this new modelling is to work with the original data
255 without using either SE energy space discretisation or polynomial approximations. For this purpose, a set of FCS operating points K_{fcs} is defined from the input data sheet ($|K_{fcs}| = 601$) that allows plotting the FCS efficiency curve. Each point $i \in K_{fcs}$ is characterised by its efficiency $\eta_{fcs}(i)$ and the power it provides $P_{fcs}(i)$. In the non-linear modelling, the power

260 losses curve $Loss_{se}(P_{se}(t))$ is identified by a polynomial approximation, using a data sheet of $|J| = 121$ points that correspond to the power losses for each power provided by the SE.

In a combinatorial approach, the power losses function is decomposed into $|J|-1$ linear functions, and J_{se} denotes the set of linear functions, which forms
 265 the power losses function. Instead of polynomial approximation classically used in methods presented in Section 3 for the HEV field, this innovative modelling is data driven and provides a combinatorial formulation. There is no use of Hessian, derivative and so on. In this framework, the new decision variables of the combinatorial modelling are:

- 270 • $X_i(t) \in \{0, 1\}$ the activation or not of the FCS operating point $i \in K_{fcs}$ at time t ,
- $Y_j(t) \in \{0, 1\}$ the activation or not of the linear function $j \in J_{se}$ to calculate the power lost at time t ,
- $P_{se}(t)$ the power provided or recovered by the SE at time t ,
- 275 • $SoE(t)$ the state of energy of the SE at time t ,
- $Eloss_{se}(t)$ the power lost by the SE at time t .

Using the new decision variables, the objective function and some constraints defined in the previous modelling change and allow the definition of a novel formulation. The objective function that minimises hydrogen consumption becomes as follows:

$$\min \sum_{t=1}^T \sum_{i=1}^{K_{fcs}} X_i(t) \frac{P_{fcs}(i)}{\eta_{fcs}(i)} \Delta t \quad (11)$$

The above objective function is optimised under the following constraints. To satisfy the vehicle powertrain demand expressed in (12), constraint (13) is imposed, which means one FCS operating point is activated at each time:

$$P_{se}(t) + \sum_{i=1}^{K_{fcs}} X_i(t) P_{fcs}(i) \geq P_{req}(t), \quad \forall t \in T, \forall i \in K_{fcs} \quad (12)$$

$$\sum_{i=1}^{K_{fcs}} X_i(t) = 1, \quad \forall t \in T, \forall i \in K_{fcs} \quad (13)$$

The second issue is how to linearise the SE power losses function. Knowing that the power losses curve (Figure 2b) is a piecewise linear convex function, it can be modelled as follows:

$$E_{loss_{se}}(t) = \alpha_j P_{se}(t) + \beta_j, \quad \forall P_{se}(t) \in [\gamma_j, \gamma'_j] \quad (14)$$

with (α_j, β_j) the characteristics of line j over interval $[\gamma_j, \gamma'_j]$. To find the quantity of power losses corresponding to the power provided/recovered by the SE (Figure 4), a new formulation is proposed using the *Max* function (Eq. 15):

$$E_{loss_{se}}(t) = \max_{j=1}^{|J_{se}|} \alpha_j P_{se}(t) + \beta_j, \quad \forall t \in T \quad (15)$$

where $|J_{se}|$ is the number of linear functions and $j \in J_{se}$ its index.

INSERT FIGURE 4 ABOUT HERE

Knowing that Max function is also non-linear, it can be modelled as a system of linear equations using binary variables and a *big-M* constant. It should be noted that M should be a high value; a too-high value would not

change the quality of the solution but it would uselessly increase computation time. So, M must be chosen carefully, in terms of the scope of the data.

$$Eloss_{se}(t) \leq \alpha_j P_{se}(t) + \beta_j + M(1 - Y_j(t)), \quad \forall t \in T, \forall j \in J_{se} \quad (16)$$

$$Eloss_{se}(t) \geq \alpha_j P_{se}(t) + \beta_j, \quad \forall t \in T, \forall j \in J_{se} \quad (17)$$

$$\sum_{j=1}^{J_{se}} Y_j(t) = 1, \quad \forall t \in T \quad (18)$$

Constraint (18) means that one and only one linear equation $\alpha_j P_{se}(t) + \beta_j$ is
 280 activated at each time t , amongst all the lines of the set J_{se} .

Remaining constraints are let unchanged: *i.e.*, energy recovery during brake phases, sources design (SE power limits and capacity), and SE energy level recovery at the end of the mission. Thus, the global novel linear model is:

$$\min \sum_{t=1}^T \sum_{i=1}^{K_{fcs}} X_i(t) \frac{P_{fcs}(i)}{\eta_{fcs}(i)} \Delta t \quad (19)$$

$$P_{se}(t) + \sum_{i=1}^{K_{fcs}} X_i(t) P_{fcs}(i) \geq P_{req}(t) \quad \forall t \in T \quad (20)$$

$$\sum_{i=1}^{K_{fcs}} X_i(t) = 1 \quad \forall t \in T \quad (21)$$

$$P_{se}^{min} \leq P_{se}(t) \leq P_{se}^{max} \quad \forall t \in T \quad (22)$$

$$SoE^{min} \leq SoE(t) \leq SoE^{max} \quad \forall t \in T \quad (23)$$

$$SoE(t) = SoE(t-1) - P_s(t) \Delta t \quad \forall t \in T \quad (24)$$

$$Eloss_{se}(t) \leq \alpha_j P_{se}(t) + \beta_j + M(1 - Y_j(t)) \quad \forall t \in T, \forall j \in J_{se} \quad (25)$$

$$Eloss_{se}(t) \geq \alpha_j P_{se}(t) + \beta_j \quad \forall t \in T, \forall j \in J_{se} \quad (26)$$

$$\sum_{j=1}^{J_{se}} Y_j(t) = 1 \quad \forall t \in T \quad (27)$$

$$P_s(t) = P_{se}(t) + Eloss_{se}(t) \quad \forall t \in T \quad (28)$$

$$SoE(T) = SoE(0) \quad (29)$$

$$X_i(t) \in \{0, 1\} \quad \forall t \in T, \forall i \in K_{fcs} \quad (30)$$

$$Y_j(t) \in \{0, 1\} \quad \forall t \in T, \forall j \in J_{se} \quad (31)$$

285 The transition to a linear modelling allows solving the problem efficiently. The discretisation of the FCS energy space and the linearisation of the SE power losses function led us to remove some constraints and introduce others by adding new decision variables. The new model contains $T(K_{fcs} + J_{se} + 3)$ variables of which $T(K_{fcs} + J_{se})$ binaries. The formulation is therefore non-compact since the number of variables is pseudo-polynomial (which may

290

cause a loss of efficiency for large horizons).

5. Results and simulations

Branch-and-Cut method refers to a hybrid method of combinatorial optimisation. It is generally employed to solve NP-hard mixed integer linear programming (MILP) problems, such as:

$$\left\{ \begin{array}{l} \min f(x) \\ g(x) \leq b \\ x \leq x^{max} \\ x \in \mathbb{Z}^n \end{array} \right.$$

The Branch-and-Cut method integrates cutting planes to accelerate the optimisation process and Branch-and-Bound methods [21]. The principle is to solve the relaxation of the integer linear problem using the Simplex algorithm, by relaxing the integrity constraints $x \in \mathbb{Z}^n \Rightarrow x \in \mathbb{R}^n$. If the solution found is feasible for the integer problem, it means that this solution is optimal; otherwise, a cutting plane method is applied in order to reduce the search space by iteratively adding cuts that violate the relaxed solution. This method also allows finding the optimal solution or accelerating the optimisation process of Branch-and-Bound method.

The Branch-and-Bound method allows solving an integer linear problem using a tree search. The principle is to separate the relaxed problem into two sub-problems (nodes) according to the fractional solution, which is integer in the master problem, and evaluate their solutions using Simplex algorithm. This process is repeated until the optimal solution is found.

310 To solve the combinatorial model, a decision tool is developed in C++
language. This tool uses the *Concert* application that calls the IBM ILOG
CPLEX mathematical optimisation solver³. Hydrogen consumption by the
fuel cell is summarised in the table below according to the mission profiles,
taking into account the optional constraint that recovers the state of energy
315 of the storage element at the end of the mission.

The results of the combinatorial approach are better and less CPU time
consuming. With regards to previous results (Table 2), it is clear than for
each profile the combinatorial optimization provides a lower consumption
(*e.g.*, ESKISEHIR uses DP = 31826 kW_s, QN = 27542 kW_s, and combina-
320 torial solution with the same constraint at the final state of charge is 27414
kW_s). Moreover, even if the final state of charge is not fixed FL = 29802
kW_s and combinatorial solution is 26924 kW_s. DP and QN solutions are
found after few hours instead of only 20 to 40 seconds for the combinatorial
problem solving.

325 INSERT TABLE 3 ABOUT HERE

Solving the novel combinatorial formulation allows reaching an optimal
decision to manage the energy distribution of the HEV sources with a re-
duced computation time, in comparison with the previously mentioned en-
ergy strategies, as shown in Table 2. In order to explain the results obtained
330 using the combinatorial modelling, simulations performed on INRETS and

³CPLEX uses Branch-and-Cut algorithm to solve integer linear problems. It is applied
to reformulate the feasible set of solutions using a pre-processing step and a cutting plane
algorithm.

ESKISEHIR mission profiles show that the fuel cell system generally operates in the maximum efficiency range to reduce the consumption of hydrogen, as shown in Figure 5. The displacement of some used set-points obtained with the new proposed combinatorial approach is sufficient to decrease the hydrogen consumption and explain the better results presented in Table 3.
335 This optimal decision corresponds to a lower (or greater) decision at some instant $k \in [1, |T|]$ contributing to a lower overall consumption.

INSERT FIGURE 5 ABOUT HERE

When the electric motor's power demand is very small, the storage element itself provides traction to the vehicle thereby minimising the consumption of hydrogen by the fuel cell. Related to power split shown in Figure 6, as soon as the demand of the electric motor reaches fairly high values, the fuel cell provides more power than the one requested by the electric motor by choosing a maximum operating efficiency point in order to minimise hydrogen consumption; surplus generated power is stored in the storage element for future use. When demand reaches high peaks, the storage element provides part of the power required, while the rest of this power is supplied by the fuel cell using an efficiency operation point that belongs to the interval where the FC is known as efficient.
340
345

350 INSERT FIGURE 6 ABOUT HERE

In Figure 6, the red curve represents the power of the fuel cell system. The continuous green curve represents the power of the storage element. The blue curve is the sum of the two previous curves and represents the total

requested charge to deliver. In the figure, each point with an asterisk (*)
355 corresponds to a time t ; all pairs of points $(P_{fcs}(t), P_{se}(t))$ over the interval
[1, $|T|$] constitute the result of the proposed combinatorial optimisation.

The inclusion of the optional constraint on the final state of energy im-
pacts the consumption of hydrogen by the fuel cell in a meaningful way:
when this constraint is activated, the fuel cell must ensure vehicle traction,
360 maintaining the state of energy between its limits and re-establishing it to its
original level at the end of the mission, with the effect of a hydrogen overcon-
sumption to charge the storage element. When this constraint is deactivated,
the fuel cell is involved only in vehicle traction and in maintaining the state
of energy between its limits, which explains the complete discharge of the
365 storage element at the end of the mission. This has the effect of reducing
requests from the fuel cell, to retain the maximum amount of hydrogen in
the tank and extending vehicle autonomy.

It is noted that the security constraints on power limitation recovered/su-
plied, $P_{se} \in [-60, 60] kW$, by the storage element are respected even in
370 braking (see the red curve in Figure 6). It is possible that the power generated
by the electric motor during braking phases is greater than the limit imposed
by the safety device. In this case, the storage element recovers possible
maximum energy and the rest is dissipated as heat in a resistor, thereby
maintaining the good functioning of the sources. Moreover, the state of
375 energy of the storage element varies, depending on the charge and discharge
mode. Charging mode corresponds to the energy recovery in braking phases
or when the fuel cell provides more power due to the low demands of the
electric motor, and this in order to minimise the consumption of hydrogen

by choosing an efficient operating point. The decrease in the state of energy
380 (discharge mode) is recognised when the power required by the motor is high,
consecutive to the participation of the storage element for vehicle traction or
when demand reaches fairly low thresholds. In this case, the storage element
itself provides the power required by the motor.

In addition, at the end of the mission, the final charge state is re-established
385 to the same level as at the beginning of the mission, in consideration of the
optional state of energy constraint, as shown in Figure 7. This is reflected
in the braking energy recovery before stopping the vehicle in order to reload
the storage element, and if the braking energy is insufficient to recover the
final state of energy, the FC is enabled for charging.

390 INSERT FIGURE 7 ABOUT HERE

To validate the linearisation of the power losses curve, Figure 8 depicts
the power losses according to the power supplied or recovered by the storage
element. It should be noted that the power losses curve used, defined by
the technical specification, matches with the power losses obtained with the
395 proposed modelling using all points on the overall SE plane of the storage
element more intensively to obtain the minimum hydrogen consumption.

INSERT FIGURE 8 ABOUT HERE

In reality, the fuel cell cannot instantaneously deliver high power (*e.g.*,
30 kW in one second) due to the functioning of its ancillaries. For this reason,
a new representative constraint (32) of the fuel cell's dynamic behaviour is
introduced, since the instantaneous power supplied between two successive

moments is limited by a boundary defined by the FC compressor type.

$$\left| \sum_{i \in K_{fcs}} X_i(t+1)P_{fcs}(i) - \sum_{i \in K_{fcs}} X_i(t)P_{fcs}(i) \right| \leq P_{fcs}^{lim} \quad \forall t \in T \quad (32)$$

which can also be expressed in the following form:

$$-P_{fcs}^{lim} \leq \sum_{i \in K_{fcs}} X_i(t+1)P_{fcs}(i) - \sum_{i \in K_{fcs}} X_i(t)P_{fcs}(i) \leq P_{fcs}^{lim} \quad \forall t \in T \quad (33)$$

The addition of this constraint in the combinatorial model necessarily will impact hydrogen consumption. When the limited power between two successive moments P_{fcs}^{lim} corresponds to the operating point that has an FCS efficient performance, previously found hydrogen consumption remains optimal. Imposing a low power limitation forces the fuel cell to use a poorer operating point, however, in order to meet the demand of the motor and of the limitation constraint (33), thus leading to overconsumption of hydrogen, as shown in Table 4.

INSERT TABLE 4 ABOUT HERE

Between two successive moments, the FCS limitation constraint added has small effects, as observed on the HIGHWAY mission profile. This is due to the motor demand, which is relatively constant and does not solicit large power variation. This is also true for the ESKISEHIR mission profile, which is a Tramway profile, in order to not agitate passengers.

It should be noted that, taking into account constraint (33) offers the possibility for fuel cell to charge the supercapacitor in the stopping phases, using an operating point that depends on the fixed power P_{fcs}^{lim} ; this may be observed, for example, in Figure 7(b) over the range [820, 870]. This choice

makes it possible to satisfy future demand of the electric motor P_{req} when $P_{req} > P_{fcs}^{lim}$. However, this constraint forces the fuel cell to use non-optimal operating points (Figure 9), which leads to a higher hydrogen consumption noted in Table 4.

420

INSERT FIGURE 9 ABOUT HERE

The combinatorial model was used to achieve optimal power management decisions with a very low computation time compared with the different strategies previously mentioned. In addition, the integration of several optional constraints on fuel cell operations or on the final state of energy
425 of the storage element allows a degree of freedom in the selection of the management strategy.

The performance of the combinatorial model in terms of solution quality and computation time can be exploited to reconfigure the pre-calculated optimal solution whenever the data change on-line due to the disruption
430 of a part of the mission profile. This situation may occur if there is a poor estimate or a detour of the mission profile that the vehicle is to achieve for any reason. In accordance with the decisions already made online by the vehicle, however, the quality of the new adjusted solution depends on the magnitude of these disturbances. Thus, one only has to re-optimize the sequence where
435 the disruption occurs by constraining the final state of energy of the new sequence so that it is the same as the state of energy of the sequence before the reconfiguration process. This condition is used to maintain the validity of the new global sequence.

6. Robustness study

440 The quality of the solutions obtained depends on the reliability of input data. Therefore, it is conceivable that the mission profile of the vehicle is obtained from an approximate calculation including some tolerance for error. In this case, it is interesting to carry out a robustness study to provide a correct and optimal solution taking into account the disrupted parameters [22].

445 In this section, uncertainties related to the mission profile of the vehicle that may be derived from an estimated calculation are considered. These uncertainties inevitably will impact the validity of the pre-calculated optimal solution found above. To deal with any eventuality that may occur, a robust linear modelling was developed to provide a worst-case robust solution [23],
450 achievable regardless of the degree of disturbance.

In order to circumvent this problem, real-time adjustment and heuristics can be implemented, using the optimal power solution obtained for the storage element $P_{se}(t), \forall t \in T$, the obtained power provided by the optimisation as reference for a bidirectional converter, and the demand of the electric motor thus ensured by the fuel cell. If at time t , engine demand is not perturbed,
455 the power supplied by the fuel cell is the same as that found by the optimisation. If not, power is deduced automatically, $P_{fcs}(t) = P_{req}(t) - P_{se}(t)$. Disruption therefore impacts the estimation of the quantity of hydrogen required to achieve the mission, which causes the vehicle to stop before the
460 end of the mission. Using robust optimisation, however, leads to a better estimation of the hydrogen quantity required for the worst-case scenario.

Assume that the demand of the electric motor is uncertain and varies in view of the information of its estimated nominal value P_{req}^{nom} and its margin

of error P_{req}^{err} . However, the actual demand of the electric motor at time t belongs to the interval $[P_{req}^{nom}(t) - P_{req}^{err}(t), P_{req}^{nom}(t) + P_{req}^{err}(t)]$, which can be expressed as:

$$P_{req}(t) = P_{req}^{nom}(t) + \epsilon_t P_{req}^{err}(t) \quad \forall \epsilon_t \in [-1, 1], t \in T \quad (34)$$

Taking into account the uncertainties represented in (34) provides optimal worst-case solution using the Soyster's approach [24]. This can be done by replacing the demand satisfaction constraint with the robust constraint (35) in the previous combinatorial model:

$$P_{se}(t) + \sum_{i \in K_{fcs}} X_i(t) P_{fcs}(i) \geq \max_{-1 \leq \epsilon_t \leq 1} \{P_{req}^{nom}(t) + \epsilon_t P_{req}^{err}(t)\} \quad \forall t \in T \quad (35)$$

It can be seen that the optimal worst-case solution is reached by fixing uncertainty values to $\epsilon_t = 1$ when electric motor demand is positive, and to $\epsilon_t = -1$ when it is negative. This implies that the mission profile is characterized by high (resp. low) power demands during the traction (resp. braking) phases:

$$P_{se}(t) + \sum_{i \in K_{fcs}} X_i(t) P_{fcs}(i) \geq P_{req}^{nom}(t) + P_{req}^{err}(t) \quad \forall t \in T, P_{req} \geq 0 \quad (36)$$

$$P_{se}(t) + \sum_{i \in K_{fcs}} X_i(t) P_{fcs}(i) \geq P_{req}^{nom}(t) - P_{req}^{err}(t) \quad \forall t \in T, P_{req} \leq 0 \quad (37)$$

Assume now that these uncertainties vary with a rate of 5%, called $\tau = 0.05$, compared to demand of the electric motor over a given time interval ($P_{req}^{err}(t) = \tau P_{req}^{nom}(t)$, $t \in [200, 399 s]$ for the INRETS mission profile, and $t \in [400, 799 s]$ for the ESKISEHIR mission profile). The optimal worst-case solution obtained using the robust formulation is expressed in Table 5.

INSERT TABLE 5 ABOUT HERE

The worst-case solution obtained is valid regardless of the realisation of scenarios belonging to the set $\{\epsilon_t \in \mathbb{R} \mid -1 \leq \epsilon_t \leq 1, \forall t \in T\}$ defined
470 above. The hydrogen consumption of the robust solution is greater than that calculated using the nominal mission profile. When the perturbation applied the demand of the electric motor is higher than its nominal demand, the fuel cell is prompted to provide more power. Or, in the braking phases, the storage element recovers less power than before, forcing the fuel cell
475 to provide the necessary power in order to avoid violating storage capacity constraints and recovering the final state of energy of the storage element at the end of the mission, if it is taken into account.

7. Conclusions

The interest of the approaches outlined in this paper is to manage the power
480 distribution of a hybrid electric vehicle. When the mission profile of the vehicle is known, offline decision strategies are relevant despite their level of criticality for real-time applications. A novel approach has been proposed to improve the quality of decisions for the Energy Management System (EMS), by modelling the energy management problem as a combinatorial optimisa-
485 tion problem after a piecewise linearisation of the curve of the power losses of the storage element (SE) and discretisation of the space of the main energy source (Fuel Cell). This transformation of the problem allowed using exact methods of operations research such as Mixed Integer Linear Program-
490 ming to solve the problem to optimality, with greatly reduced computation times. Other constraints were introduced and simulated in order to closely

reproduce the real functioning of the primary source, *i.e.*, power limiting constraints per time step.

To measure the sensitivity of the issue against disturbances related to the demand of the electric motor, a robust study is conducted based on the
495 Soyster's robust approach to guarantee that a worst-case solution will be valid regardless of the scenario.

A novel combinatorial approach is proposed for the first time in the field of this electric hybrid structure. Compared to other methods, the propositions turn out to be very efficient, in terms of low energy consumption, time
500 needed to optimally compute power split and overall energy management. A real-time application is possible when the time step is large (few seconds) to control the energy distribution of the vehicle.

The robustness study presented in this paper concerns disruption of the demand. Analysis of the sensitivity of the combinational model by disrupt-
505 ing the energy sources characteristics (FC efficiency and power losses of the storage element) is suggested thus. Application of the parametric approach of Bertsimas and Sim is interesting in this case, because it gives the different worst-case consumption according to the disruption level, which is controlled by a disruption factor.

510 **References**

- [1] A. Emadi, S. S. Williamson, Modern automotive power systems: Advancements into the future, in: Power Electronics and Motion Control Conference, 2006. EPE-PEMC 2006. 12th International, IEEE, 2006, pp. 1762–1768.

- 515 [2] R. van den Hoed, Commitment to fuel cell technology? how to interpret
carmakers' efforts in this radical technology, *Journal of power sources*
141 (2) (2005) 265–271.
- [3] J. P. Trovão, P. G. Pereirinha, H. M. Jorge, C. Henggeler Antunes,
A multi-level energy management system for multi-source electric vehi-
520 cles – An integrated rule-based meta-heuristic approach, *Applied Energy*
105 (2013) 304–318.
- [4] T. Sousa, Z. Vale, J. P. Carvalho, T. Pinto, H. Morais, A hybrid sim-
ulated annealing approach to handle energy resource management con-
sidering an intensive use of electric vehicles, *Energy* 67 (2014) 81–96.
- 525 [5] L. V. Pérez, G. R. Bossio, D. Moitre, G. O. García, Optimization of
power management in a hybrid electric vehicle using dynamic program-
ming, *Mathematics and Computers in Simulation* 73 (1) (2006) 244–254.
- [6] M. Guemri, S. Caux, S. U. Ngueveu, F. Messine, Heuristics and lower
bound for energy management in hybrid-electric vehicles, in: *Proceed-*
530 *ings of the 9th International Conference on Modeling, Optimization and*
Simulation (MOSIM), Bordeaux, 2012.
- [7] S. Delprat, T.-M. Guerra, J. Rimaux, Optimal control of a parallel pow-
ertrain: from global optimization to real time control strategy, *IEEE*
Transactions on Vehicular Technology 53 (3) (2004) 872–881.
- 535 [8] A. Sciarretta, M. Back, L. Guzzella, Optimal control of parallel hy-
brid electric vehicles, *IEEE Transactions on Control Systems Technology*
12 (3) (2004) 352–363.

- [9] J. P. Gao, G. M. G. Zhu, E. G. Strangas, F. C. Sun, Equivalent fuel consumption optimal control of a series hybrid electric vehicle, in: Proceedings of the Institution of Mechanical Engineers, Part D: Journal of Automobile Engineering, Vol. 223, Sage Publications, 2009, pp. 1003–1018.
- [10] S. Caux, D. Wanderley-Honda, D. Hissel, M. Fadel, On-line energy management for HEV based on particle swarm optimization, The European Physical Journal Applied Physics (2010) 1–7.
- [11] L. Serrao, S. Onori, G. Rizzoni, ECMS as a realization of Pontryagin’s minimum principle for HEV control, in: Proceedings of the American Control Conference, IEEE, 2009, pp. 3964–3969.
- [12] C. Musardo, G. Rizzoni, Y. Guezennec, B. Staccia, A-ECMS: An adaptive algorithm for hybrid electric vehicle energy management, European Journal of Control 11 (4) (2005) 509–524.
- [13] N. J. Schouten, M. A. Salman, N. A. Kheir, Energy management strategies for parallel hybrid vehicles using fuzzy logic, Control Engineering Practice 11 (2) (2003) 171–177.
- [14] A. Neffati, M. Guemri, S. Caux, M. Fadel, Energy management strategies for multi source systems, Electric Power Systems Research 102 (2013) 42–49.
- [15] S. Caux, W. Hankache, M. Fadel, D. Hissel, On-line fuzzy energy management for hybrid fuel cell systems, International Journal of Hydrogen Energy 35 (5) (2010) 2134–2143.

- [16] H. Khayyam, A. Bab-Hadiashar, Adaptive intelligent energy management system of plug-in hybrid electric vehicle, *Energy* 69 (2014) 319–335.
- [17] N. Bizon, M. Radut, M. Oproescu, Energy control strategies for the fuel cell hybrid power source under unknown load profil, *Energy* 86 (2015) 31–41.
- [18] R. K. Ahluwalia, X. Wang, A. Rousseau, R. Kumar, Fuel economy of hydrogen fuel cell vehicles, *Journal of Power Sources* 130 (1) (2004) 192–201.
- [19] K. T. Chau, C. C. Chan, Emerging energy-efficient technologies for hybrid electric vehicles, *Proceedings of the IEEE* 95 (4) (2007) 821–835.
- [20] R. L. Rardin, *Optimization in operations research*, Vol. 166, Prentice Hall, New Jersey, 1998.
- [21] W. L. Winston, *Operations research: applications and algorithms*, (third ed.) Duxbury press, Belmont, California, 1994.
- [22] D. Bertsimas, D. B. Brown, C. Caramanis, Theory and applications of robust optimization, *SIAM Review* 53 (3) (2011) 464–501.
- [23] A. L. Soyster, Inexact linear programming with generalized resource sets, *European Journal of Operational Research* 3 (4) (1979) 316–321.
- [24] A. L. Soyster, Convex programming with set-inclusive constraints and applications to inexact linear programming, *Operations Research* 21 (5) (1973) 1154–1157.

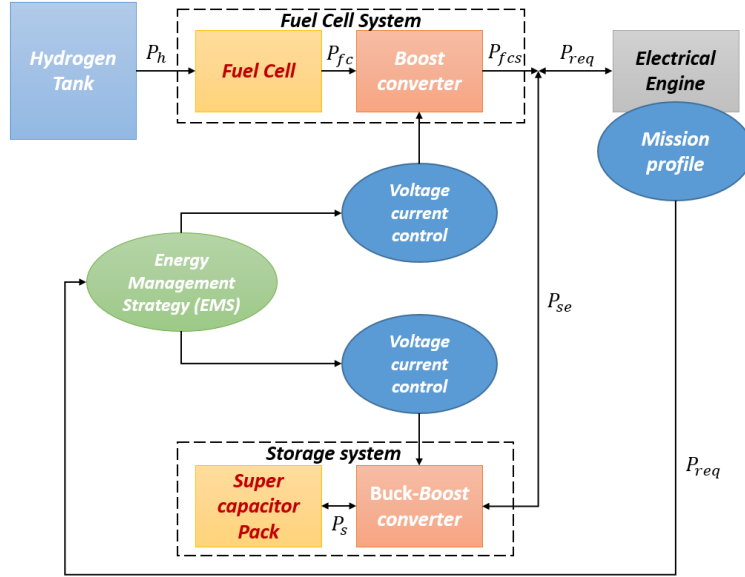
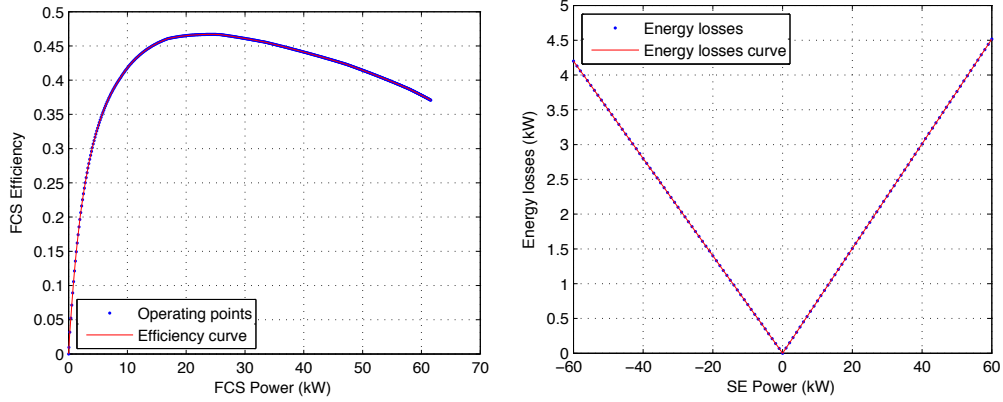


Figure 1: HEV Energy System.



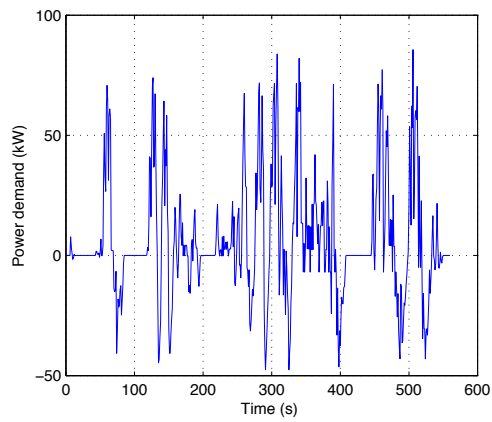
(a) Fuel cell system efficiency.

(b) Energy losses of the storage system.

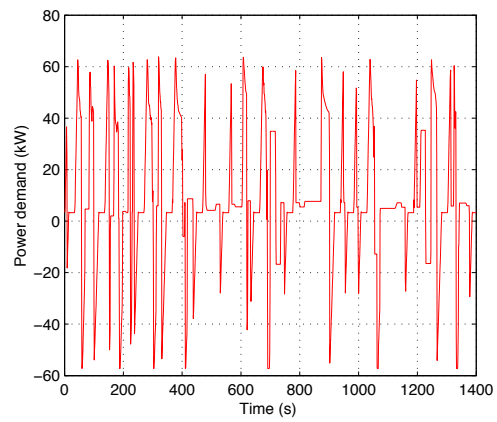
Figure 2: Characteristics of the energy sources.

Table 1: Input data.

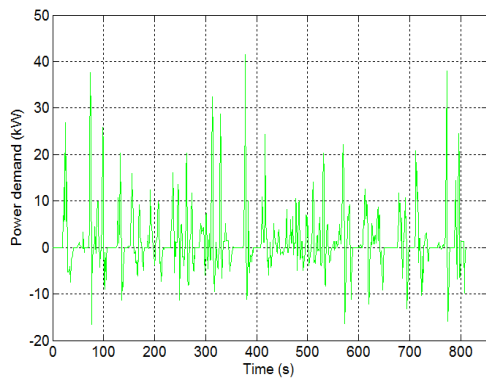
Notation	Value	Definition
SoE^{max}	100% ($E_{nom} = 1600 \text{ kW s}$)	Maximum energy storable in SE
SoE^{min}	25% (400 kW s)	Minimum energy storable in SE
$SoE(0)$	56.25% (900 kW s)	Initial energy storable in SE
P_{se}^{min}	-60 kW	Minimum power injected to SE
P_{se}^{max}	60 kW	Maximum power extractable from SE
P_{fcs}^{max}	70 kW	Maximum power extractable from FCS
Δt	1 s	Time stepsize
T		Mission duration



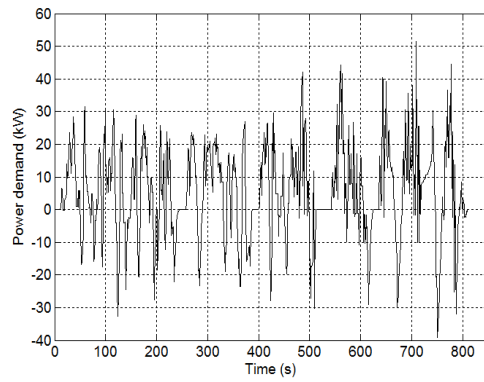
(a) INRETS mission profile over 560 s.



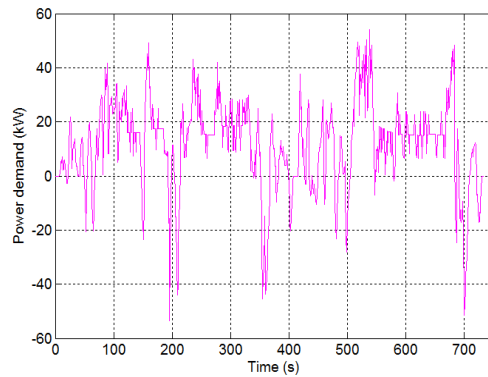
(b) ESKISEHIR mission profile over 1400 s.



(c) Urban mission profile over 811 s.



(d) Road mission profile over 811 s.



(e) Highway mission profile over 734 s.

Figure 3: Mission profiles used in the simulation.

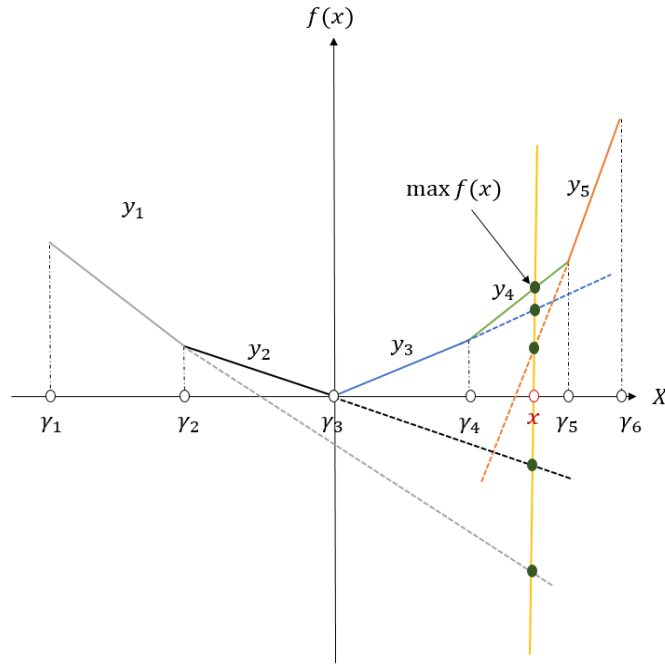


Figure 4: Linearisation of convex function.

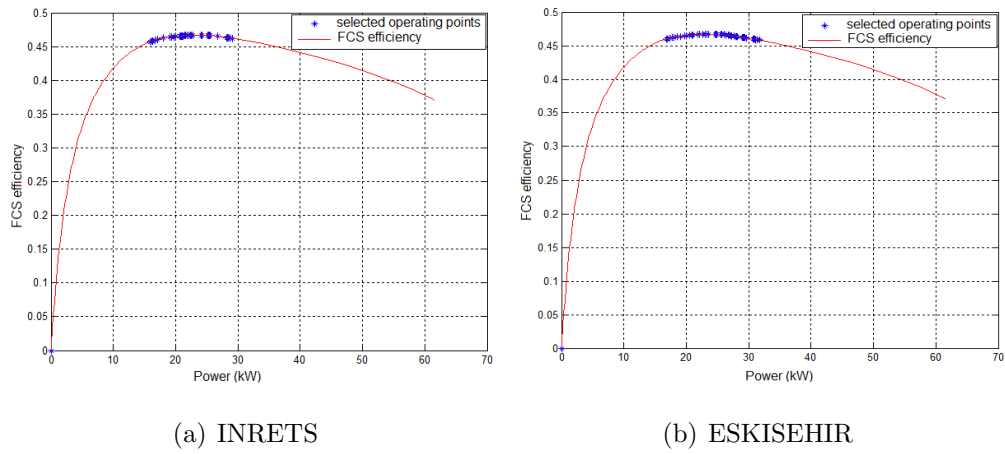
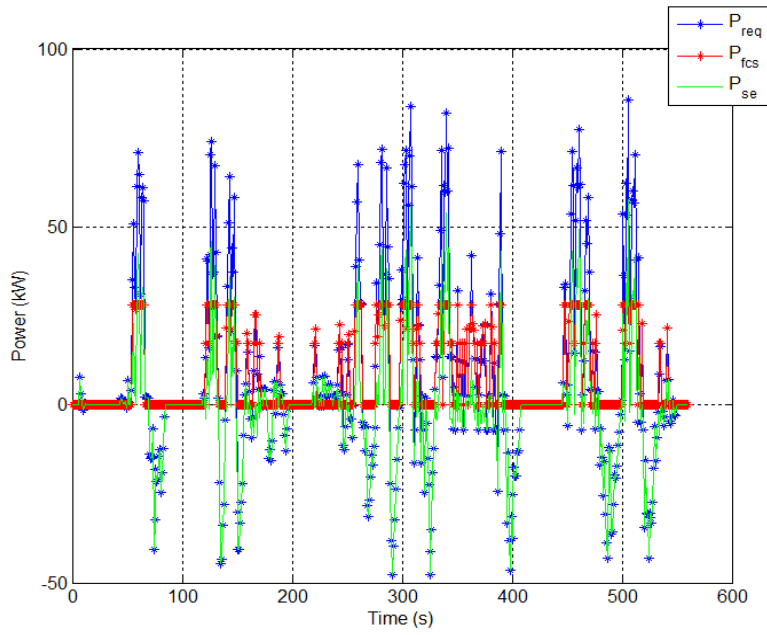
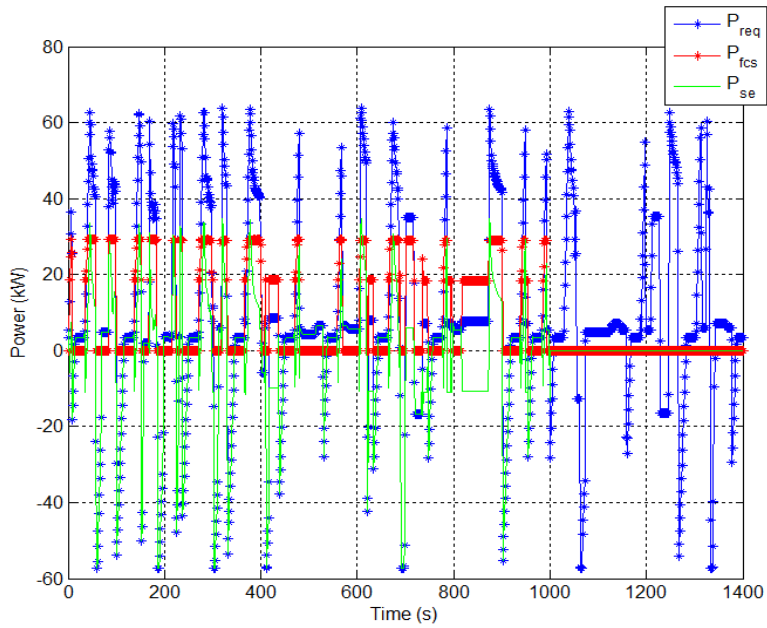


Figure 5: Selected FCS operating points.

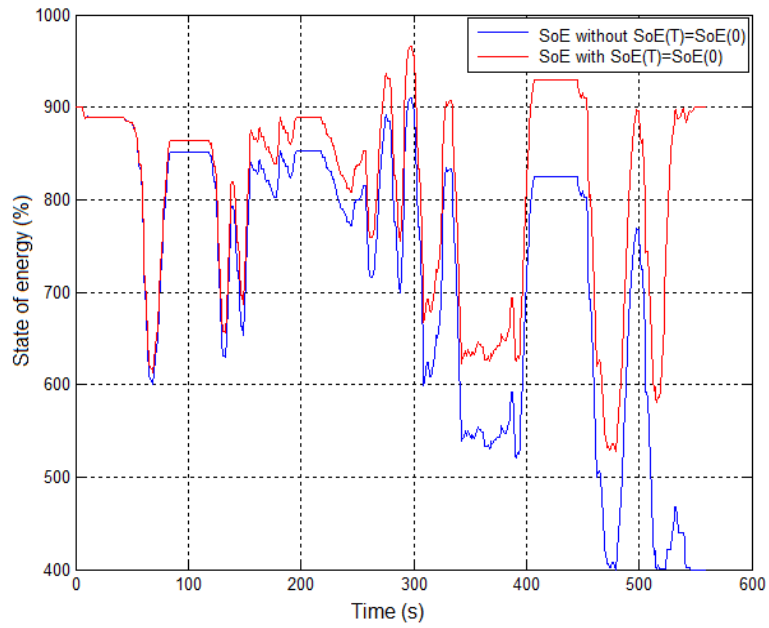


(a) INRETS

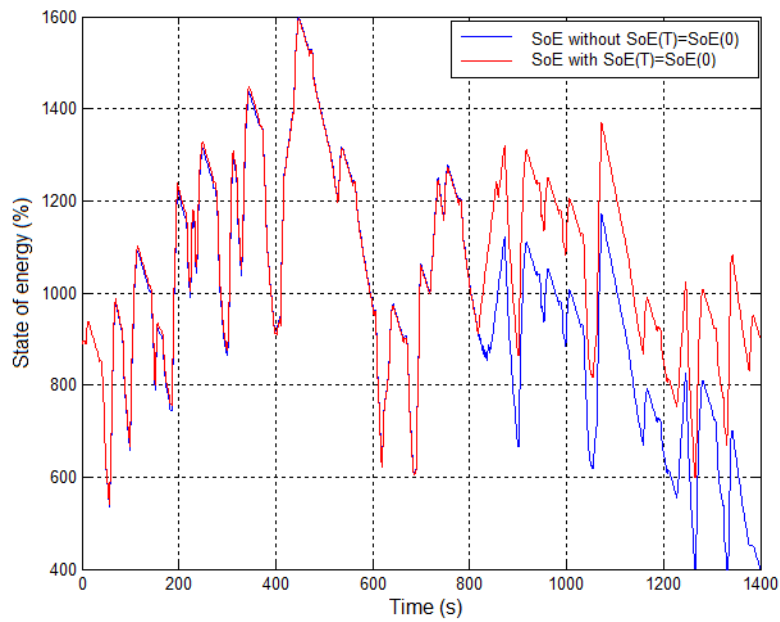


(b) ESKISEHIR

Figure 6: Powers provided by the sources (P_{fcs} , P_{se}) and the demand (P_{req}).

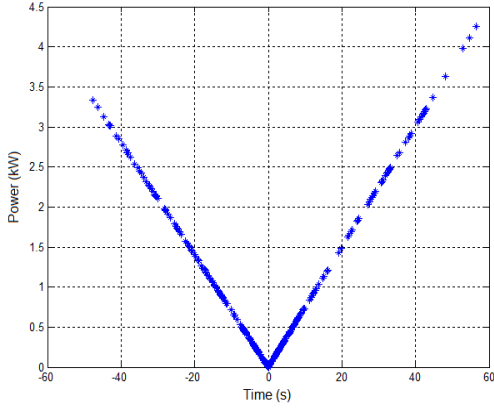


(a) INRETS

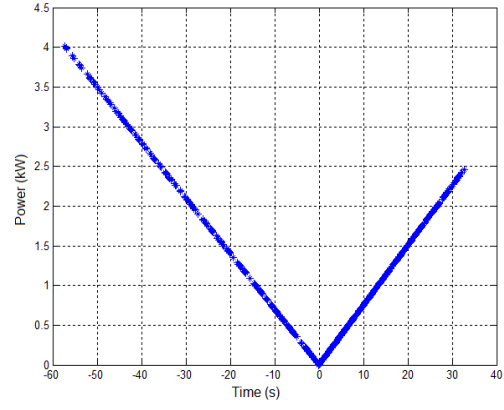


(b) ESKISEHIR

Figure 7: SE available Energy.

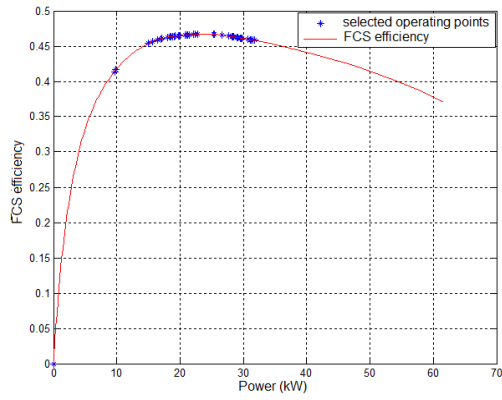


(a) INRETS

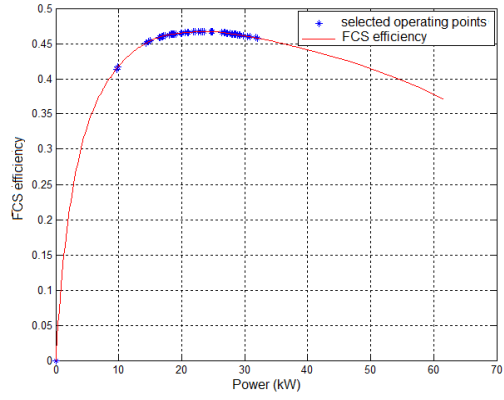


(b) ESKISEHIR

Figure 8: Energy losses by the storage element.



(a) INRETS



(b) ESKISEHIR

Figure 9: Selected operating points by the fuel cell when the limitation constraint, $P_{fcs}^{lim} = 10 \text{ kW}$, is activated.

Table 2: Non-linear programming problem solution.

Mission profile	Approach	Hydrogen		
		consumption	CPU Time	$SoE(T) = SoE(0)?$
INRETS	QN	8750 kWs	23 <i>mn</i>	Yes
	FL	8359 kWs	<i>Real Time</i>	No
	DP	9189.7 kWs	48 <i>h</i>	Yes
ESKISEHIR	QN	27542 kWs	2.4 <i>h</i>	Yes
	FL	29802 kWs	<i>Real Time</i>	No
	DP	31826 kWs	52 <i>h</i>	Yes
URBAN	QN	2954 kWs	78 <i>min</i>	Yes
	FL	3390.2 kWs	<i>Real Time</i>	No
	DP	5986 kWs	44 <i>h</i>	Yes
ROAD	QN	10467 kWs	80 <i>min</i>	Yes
	FL	11031 kWs	<i>Real Time</i>	No
	DP	12669 kWs	44 <i>h</i>	Yes
HIGHWAY	QN	19016 kWs	84 <i>min</i>	Yes
	FL	19710 kWs	<i>Real Time</i>	No
	DP	20099 kWs	48 <i>h</i>	Yes

Table 3: Results obtained by solving the combinatorial modelling with CPLEX 12.4

Mission profile	Hydrogen consumption	CPU Time	$SoE(T) = SoE(0)?$
INRETS	8750 kWs	3 s	Yes
	8269 kWs	5 s	No
ESKISEHIR	27514.2 kWs	26 s	Yes
	26924 kWs	45 s	No
URBAN	2615.95 kWs	24 s	Yes
	1598.3 kWs	67 s	No
ROAD	9704.42 kWs	17 s	Yes
	8892.1 kWs	23 s	No
HIGHWAY	18601.4 kWs	10 s	Yes
	18333.4 kWs	11 s	No

Table 4: Results obtained by solving the combinatorial modelling with CPLEX 12.4 in addition of limitation constraint between two successive moments Δt .

Mission profile	Hydrogen consumption	CPU time	$SoE(T) = SoE(0)?$
INRETS	8966.07 <i>kWs</i>	393 <i>s</i>	Yes
	8462.37 <i>kWs</i>	209 <i>s</i>	No
ESKISEHIR	27729.7 <i>kWs</i>	20 <i>min</i>	Yes
	27112.6 <i>kWs</i>	15 <i>min</i>	No
URBAN	2725.94 <i>kWs</i>	158 <i>s</i>	Yes
	1683.69 <i>kWs</i>	73 <i>s</i>	No
ROAD	9896.39 <i>kWs</i>	171 <i>s</i>	Yes
	9074.16 <i>kWs</i>	554 <i>s</i>	No
ROAD	18728.4 <i>kWs</i>	118 <i>s</i>	Yes
	18462.8 <i>kWs</i>	150 <i>s</i>	No

Table 5: Obtained results with the robust formulation.

Mission profile	Hydrogen consumption	CPU time	$SoE(T) = SoE(0)?$
INRETS	9061 kWs	4 s	Yes
	8561.33 kWs	4 s	No
ESKISEHIR	28228.1 kWs	25 s	Yes
	27639.7 kWs	24 s	No

Nomenclature

ϵ_t	time-varying uncertainty value (in $[-1, 1]$) on the power demand
$\eta_{compressor}$	air compressor efficiency
η_{cvs}	buck-boost converter efficiency embedded in the fuel cell stack
η_{fcs}	Fuel Cell Stack efficiency
η_{fc}	core hydrogen cell efficiency
E_{nom}	storage capacity of the SE
$E_{loss_{se}}$	power losses of the SE (combinatorial approach)
I_{sc}	current flowing through the super-capacitors pack
J_{se}	set of linear functions approaching SE power losses
K_{fcs}	set of FCS operating points
$Loss_{cvs}$	buck-boost SE converter efficiency
$Loss_{se}$	power losses of the SE (non-linear approach)
M	big constant
P_h	equivalent hydrogen power to minimise
P_s	real power provided or recovered by the SE
$P_{fcs}^{(max)}$	(maximum) power provided by the FCS
P_{fcs}^{lim}	limited FCS power between two successive moments
P_{req}	demand of the electric motor
P_{req}^{err}	margin of error of the demand of the electric motor
P_{req}^{nom}	initial demand of the electric motor (robust approach)
$P_{se}^{(min/max)}$	(minimum/maximum) power provided or recovered by the SE
R_{sc}	equivalent resistor of the super-capacitor pack
SoE	state of energy of the SE
T	mission duration
t	time
X_i	binary variable on the activation of the FCS operating point $i \in K_{fcs}$
Y_j	binary variable on the activation of the linear function $j \in J_{se}$ to calculate the power lost
(α_j, β_j)	parameters of line j